Ag/AgCl-Loaded Ordered Mesoporous Anatase for Photocatalysis

Martin Andersson,*[,†,‡] Henrik Birkedal,[†,§] Nathan R. Franklin,[†] Todd Ostomel,[†] Shannon Boettcher,[†] Anders E. C. Palmqvist,[‡,⊥] and Galen D. Stucky*[,†,∥]

Department of Chemistry and Biochemistry and Materials Department, University of California, Santa Barbara, California 93106-9510, and Materials and Surface Chemistry and Competence Centre for Catalysis, Chalmers University of Technology, SE-412 96 Göteborg, Sweden

Received August 25, 2004. Revised Manuscript Received December 23, 2004

Thin films of ordered mesoporous anatase have been prepared using a dip-coating procedure. Silver nanoparticles were introduced into the mesopores using wet impregnation followed by heat treatment. The cubic structured mesoporous titania had higher stability than the hexagonal structure and could be formed with a high content of nanocrystalline anatase with conservation of the meso-order. The high crystallite content was monitored by both X-ray diffraction and electron diffraction together with dark field transmission electron microscopy (TEM). The meso-order was studied using low-angle X-ray diffraction and TEM. The incorporated silver was formed within the mesopores of the titania, which acted as a template for the silver nanoparticles. X-ray photoelectron spectroscopy showed that both anatase and silver were present on the surface of the silver-loaded mesoporous titania. The synthesized titania films were evaluated for their photocatalytic activity for oxidation of stearic acid. It was found that the meso-ordered titania had a sufficiently high crystallite content to be photoactive and that the reaction mechanism resembled that of a non-meso-ordered titania sample. Upon incorporation of silver nanoparticles an apparent difference in reaction mechanism was found together with a higher apparent initial activity.

Introduction

During the past decade various catalytic techniques have been investigated to address the increasing problem of environmental pollution. One technique that has shown great potential for decomposing organic contaminants in both air and water is photocatalysis. There are several advantages of the photocatalytic approach, including that the organic contaminants can be completely decomposed to CO_2 and H_2O and that UV irradiation is used as energy input from either artificial or solar sources, making it possible for the reactions to proceed at lower temperatures. This technique has gained much attention in purification of wastewater from households and industry.[1−4] The use of the wide-band-gap semiconductor titania (TiO_2) as photocatalyst has proven attractive since this material has a high efficiency and low cost and is environmentally sustainable.[5−7] Titania exists as three different crystalline structures, anatase, rutile, and brookite, among which rutile is the most thermodynamically stable polymorph, while anatase and brookite are metastable.[8] However, the stability of the structures appears to be size-dependent, and at particle sizes below 14 nm anatase is more stable than rutile.[9,10] Anatase has a wider band gap than rutile and a redox potential that often is more suitable for practical use in photocatalysis. Rutile, on the other hand, has a larger refractive index and a higher electrical resistance, making it useful in other applications. Both anatase and rutile have proven to be photocatalytically active for decomposition of phenol, but via different reaction mechanisms, giving different intermediates upon degradation of the organic compound.[11] Degussa P-25, which is a commercially available titania formulation, has proven to be a particularly successful photocatalyst. This is believed to be due to the fact that Degussa P-25 is a mixture of anatase (80%) and rutile (20%) and that it has a high specific surface area of approximately 50 m^2/g.[12] It has been shown that this combination of polymorphs improves the stability of photogenerated electrons and hence increases the lifetime of the electron−hole pairs, resulting in higher photocatalytic activity.[13,14] Similarly, noble metals can be added to the semiconductor surface and

* To whom correspondence should be addressed. E-mail: martina@chem.chalmers.se (M.A.); stucky@chem.ucsb.edu (G.D.S.).
† Department of Chemistry and Biochemistry, University of California.
‡ Materials and Surface Chemistry, Chalmers University of Technology.
§ Present address: Department of Chemistry, University of Aarhus, Langelandsgade 140, DK-8000 Aarhus C, Denmark.
∥ Materials Department, University of California.
⊥ Competence Centre for Catalysis, Chalmers University of Technology.

(1) Serpone, N.; Maruthamuthu, P.; Pichat, P.; Pelizzetti, E.; Hidaka, H. J. *J. Photochem. Photobiol., A* **1995**, *85*, 247.
(2) Ollis, D. F.; Al-Ekabi, H. *Photocatalytic Purification and Treatment of Water and Air*; Elsevier: Amsterdam, 1993.
(3) Hoffman, M. R.; Martin, S. T.; Choi, W.; Bahnemann, D. W. *Chem. Rev.* **1995**, *95*, 69.
(4) Baird, C. *Environmental Chemistry*; Freeman: New York, 1998.
(5) Kamat, P. V. *Chem. Rev.* **1993**, *93*, 267.
(6) Pelizzetti, E.; Serpone, N. *Homogeneous and Heterogeneous Photocatalysis*; Reidel: Dordrecht, The Netherlands, 1986.
(7) Chiavello, M. *Photocatalysis and Environment, Trends and Applications*; Dordrecht, The Netherlands, 1988.
(8) Gopal, M.; Moberly, W. J.; Chan, L. C.; Jonghe, J. *J. Mater. Sci.* **1997**, *32*, 6001.
(9) Zhang, H.; Banfield, J. F. *J. Phys. Chem. B* **2000**, *104*, 3481.
(10) Zhang, H.; Banfield, J. F. *J. Mater. Chem.* **1988**, *8*, 2073.
(11) Andersson, M.; Österlund, L.; Ljungström, S.; Palmqvist, A. *J. Phys. Chem. B* **2002**, *106*, 10674.
(12) Saadoun, L.; Ayllón, J. A.; Jeménez-Becerril, J.; Doménech, X.; Rodríguez-Clemente, R. *Appl. Catal., B* **1999**, *21*, 269.
(13) Abe, R.; Sayama, K.; Domen, K.; Arakawa, H. *Chem. Phys. Lett.* **2001**, *334*, 339.
(14) Yu, J. C.; Yu, J.; Ho, W.; Zhang, L. *Chem. Commun.* **2001**, 1942.

10.1021/cm0485761 CCC: $30.25
Published on Web 02/18/2005

thereby changing the photocatalytic process.[15] The mechanism for the improvement is enhanced electron migration from the semiconductor surface to the metal, which suppresses electron−hole recombination. Silver deposition on titania has in both reduction[16,17] and oxidation[18−23] reactions proven to increase the photocatalytic activity, especially if silver is present in the form of nanoparticles.[15]

In 1992 researchers at Mobil Oil[24,25] showed that it was possible to form ordered mesoporous silica and that it was possible to produce it with different structures, e.g., hexagonal (MCM-41), cubic (MCM-48), and lamellar (MCM-50). These systems were later extended to larger pore structures by the use of amphiphilic block copolymers (SBA-*n*).[26] Since then, large efforts have been made by many research groups, both in the preparation of materials with different pore sizes and in the synthesis of materials other than silica. Transition-metal oxides have been especially in focus[27] due to their anticipated unique properties, and there are several nice reviews on the subject.[28−30] Mesoporous titania is an interesting material for photocatalytic applications. One reason for this is the very high specific surface area of these materials. Furthermore, the material is continuous, which may be beneficial compared to separated individual nanoparticles, in particular for catalyst recovery. The reasons for the low number of studies made on ordered mesoporous titania as a photocatalyst are likely related to the difficulties in making it as an ordered material. Ever since Antonelli et al.[31] first synthesized mesoporous titania in 1995, many efforts have been made to control the crystallization and to make more crystalline material with maintenance of mesoscale order. Another approach to titania-containing mesoporous materials for photocatalysis has been to modify existing mesoporous silica with titania. This has given good results and hence made it even more interesting to prepare ordered mesoporous (highly) crystalline titania.[32,33] Very few studies exist on the use of mesoporous titania for photocatalytic reactions, and these have been restricted to materials without long-range meso-order or with no to very few crystallites present.[34−37]

In this work highly ordered mesoporous titania thin films with relatively high anatase nanocrystal content have been synthesized. To increase the photocatalytic activity, silver nanoparticles have been incorporated into the mesopores of the titania. Both hexagonal and cubic mesoporous titania have been synthesized and characterized. The materials have been tested for photocatalytic activity for the degradation of stearic acid, a common organic substance used for this purpose.[38−40] Both the influence of the ordering together with the crystallinity and the influence of the silver have been evaluated.

Experimental Section

Materials. Pluronic P123, a poly(ethylene oxide)−poly(propylene oxide)−poly(ethylene oxide) block copolymer ($EO_{20}PO_{70}EO_{20}$), was received as a gift from BASF Corp. and used as the structure-directing agent. Concentrated hydrochloric acid (37.8 M), titanium(IV) tetraethoxide (95%), and $AgNO_3$ (99.8%) were all purchased from Aldrich and used as received. The ethanol used was of 200 proof purity.

Formation of Mesoporous Titania Thin Films. *Cubic Mesoporous Titania*. Cubic mesoporous titania thin films were prepared following the method of Alberius et al.[41] Briefly, the procedure can be described as follows. A 1 g sample of Pluronic P123 was dissolved in 12 g of ethanol (magnetic stirrer, 1 h). Separately, 4.2 g of titanium ethoxide was plunged into 3.2 g of hydrochloric acid using a syringe needle, and the mixture was stirred vigorously for 10 min, resulting in a clear solution. Care was taken to prevent the ethoxide from coming into contact with air. The two mixtures were then mixed together and stirred for 3 h. Glass or quartz slides were dip coated into the titanium solution using a home-built dip coater. The slides were dipped into the solution and withdrawn into open air with a pulling rate of 1 mm/s. The slides were then positioned horizontally and dried at room temperature in air for 24 h, thereby allowing most of the solvents and hydrochloric acid to evaporate and the surfactant to self-organize. The dried film was heated with a rate of 1 °C /min in stagnant air to 400 °C where it was kept for 4 h before cooling.

Hexagonal Mesoporous Titania. The same procedure as for cubic titania was used, but with 2.3 g of Pluronic P123 instead of 1 g and with a highest calcination temperature of 250 °C instead of 400 °C. The lower maximum temperature was used to avoid loss of long-range meso-order.

Incorporation of Silver into Mesoporous Titania. Silver nanoparticles were incorporated into the mesoporous titania by *in situ* heat-induced reduction after impregnation of the films in a Ag(I)-containing solution. A 50 mL solution containing 1.7 g of

(15) Linsebigler, A. L.; Guangquan, L.; J. T. Yates, J. *Chem. Rev.* **1995**, *95*, 735.
(16) Tada, H.; Teranishi, K.; Inubushi, Y.; Ito, S. *Chem. Commun.* **1998**, 2345.
(17) Tada, H.; Teranishi, K.; Inubushi, Y.; Ito, S. *Langmuir* **2000**, *16*, 3304.
(18) Zhang, L.; Yu, J. C.; Yip, H. Y.; Li, Q.; Kwong, K. W.; Xu, A.; Wong, P. K. *Langmuir* **2003**, *19*, 10372.
(19) Szabó-Bárdos, E.; Czili, H.; Horváth, A. *J. Photochem. Photobiol., A* **2003**, *154*, 195.
(20) Arabatzis, I. M.; Stergiopoulos, T.; Bernard, M. C.; Labou, D.; Neophytides, S. G.; Falaras, P. *Appl. Catal., B* **2003**, *42*, 187.
(21) Dobosz, A.; Sobczy'nski, A. *Water Res.* **2003**, *37*, 1489.
(22) He, C.; Yu, Y.; Hu, X.; Larbot, A. *Appl. Surf. Sci.* **2002**, *200*, 239.
(23) Liu, Y.; Liu, C.; Rong, Q.; Zhang, Z. *Appl. Surf. Sci.* **2003**, *220*, 7.
(24) Kresge, C. T.; Leonowicz, M. E.; Roth, W. J.; Vartuli, J. C.; Beck, J. S. *Nature* **1992**, *359*, 71.
(25) Beck, J. S.; Vartuli, J. C.; Roth, W. J.; Leonowicz, M. E.; Kresge, C. T.; Schmitt, K. D.; Chu, C. T.-W.; Olson, D. H.; Sheppard, E. W.; McCullen, S. B.; Higgins, J. B.; Schlenker, J. L. *J. Am. Chem. Soc.* **1992**, *114*, 834.
(26) Zhao, D.; Feng, J.; Huo, Q.; Melosh, N.; Fredrickson, G. H.; Chmelka, B. F.; Stucky, G. D. *Science* **1998**, *279*, 548.
(27) Yang, P.; Zhao, D.; Margolese, D. I.; Chmelka, B. F.; Stucky, G. D. *Nature* **1998**, *396*.
(28) Yu, C.; Tian, B.; Zhao, D. *Curr. Opin. Solid State Mater. Sci.* **2003**, *7*, 191.
(29) Ying, J. Y.; Mehnert, C. P.; Wong, M. S. *Angew. Chem., Int. Ed.* **1999**, *38*, 56.
(30) Palmqvist, A. E. C. *Curr. Opin. Colloid Interface Sci.* **2003**, *8*, 145.
(31) Antonelli, D. M.; Ying, J. Y. *Angew. Chem., Int. Ed.* **1995**, *34*, 2014.
(32) Belhekar, A. A.; Awate, S. V.; Anand, R. *Catal. Commun.* **2002**, *3*, 453.
(33) Zheng, S.; Gao, L.; Zhang, Q.; Guo, J. *J. Mater. Chem.* **2000**, *10*, 723.
(34) Yu, J. C.; Yu, J.; Zhao, J. *Appl. Catal., B* **2002**, *36*, 31.
(35) Yusuf, M. M.; Imai, H.; Hiraschima, H. *J. Sol-Gel Sci. Technol.* **2001**, *25*, 65.
(36) Dai, Q.; Shi, L. Y.; Luo, Y. G.; Blin, J. L.; Li, D. J.; Yuan, C. W.; Su, B. L. *J. Photochem. Photobiol., A* **2002**, *148*, 295.
(37) Stathatos, E.; Petrova, T.; Lianos, P. *Langmuir* **2001**, *17*, 5025.
(38) Minabe, T.; Tryk, D. A.; Sawunyama, P.; Kikuchi, Y.; Hashimoto, K.; Fujishima, A. *J. Photochem. Photobiol., A* **2000**, *137*, 53.
(39) Sawunyama, P.; Jiang, L.; Fujishima, A.; Hashimoto, K. *J. Phys. Chem. B* **1997**, *101*, 11000.
(40) Mills, A.; Hill, G.; Bhopal, S.; Parkin, I. P.; O'Neill, S. A. *J. Photochem. Photobiol., A* **2003**, *160*, 185.
(41) Alberius, P. C. A.; Frindell, K. L.; Hayward, R. C.; Kramer, E. J.; Stucky, G. D.; Chmelka, B. F. *Chem. Mater.* **2002**, *14*, 3284.

$AgNO_3$ dissolved in a mixture containing H_2O and ethanol (1:1 v/v) was prepared. This solvent mixture has proven to be suitable for wetting mesoporous silica.[42] The slides were impregnated with the silver solution (three per 50 mL) and kept in darkness for 24 h. During this time the hexagonal films became successively darker and finally were black, indicating the formation of metallic silver on or in the pores of the titania. The cubic titania turned light gray during the procedure. The slides were rinsed in water, removing all silver not adsorbed on or in the pores of the titania, heat treated in a tube furnace under flowing nitrogen at a rate of 1 °C/min to 300 °C, and kept there for 2 h. During this stage the cubic titania samples also turned black; no change in color was observed for the hexagonal sample.

Characterization. Low-angle as well as conventional powder X-ray diffraction (XRD) measurements were performed using a Scintag X2 (Cu Kα radiation, $\lambda = 1.54$ Å). The X-ray diffraction at higher angles was collected on samples scraped off from several slides to improve the signal-to-noise ratio. Rietveld refinement was performed against the conventional powder data using GSAS.[43] Three phases were included: AgCl, cubic Ag, and anatase TiO_2. The refinement included the lattice parameters of all phases, the phase weight fractions, isotropic displacement parameters of Ag and AgCl, and a zero point. The reflection profiles were modeled by Lorentzian size broadening, while the background was modeled by a 16-term shifted Chebyschev polynomial. The anatase atomic positions and anisotropic displacement parameters were fixed at the neutron powder diffraction values of Howard et al.[44] The final agreement indices were, for the whole pattern, wRp = 0.0390, Rp = 0.0308, and $\chi^2 = 1.344$ for 30 variables. The refined weight fractions were 73.61% anatase, 20.55(18)% AgCl, and 5.8(3)% Ag. The apparent average crystallite sizes obtained from the refinement were 15.06(12), 63.3(5), and 12.6(4) nm for anatase, AgCl, and Ag, respectively, assuming a value of 0.9 for the Scherrer constant. Note that the su's given for these numbers only reflect the precision with which they are determined by the Rietveld refinement and not the width of the particle size distribution.

An FEI Tecnai G2 Sphera transmission electron microscope operating at 200 kV was used for imaging and electron diffraction. Transmission electron microscopy (TEM) specimens were prepared by scraping of the films with a razorblade, dispersing the powder in ethanol, and placing a drop of the dispersion onto a holey carbon grid followed by drying at room temperature. Scanning electron micrographs were obtained with an FEI XL40 Sirion FEG digital scanning microscope operating at 2−5 kV.

X-ray photoelectron Spectroscopy (XPS) measurements were performed on a Kratos Axis Ultra XPS system using monochromated Al Kα radiation to explore the elements on the surface. Three films were investigated: a "cubic" film, a "hexagonal" film, and a "hexagonal" film with incorporated silver nanoparticles. Survey scans were performed using 0.5 eV steps, and high-resolution scans using 0.1 eV steps were made at the Ti 2p and Ag 3d peaks. The relative energy scale was fixed with C 1s. This showed that the Ti 2p signal occurred at the same energy in all spectra. The Ti 2p signal was then used to fix the absolute energy scale by using the Ti $2p_{3/2}$ binding energy of Ti^{4+} of 458.5 eV.

Photocatalytic Experiment. To test the photocatalytic activity of the prepared materials, the samples, which were scraped from several films, were put in stearic acid solution (0.3 g of stearic acid in 10.6 mL of chloroform) for several minutes and then heat treated in stagnant air in a furnace at 80 °C for 2 h. With this procedure the stearic acid melts and impregnates the titania, and upon cooling, a loaded dry catalyst powder is obtained. This procedure has proven suitable for the evaluation of photocatalytic activity of titania powders.[45] The photocatalytic experiment was performed using a sandwich-like microreactor consisting of a silicon plate covered by a quartz window separated by 75 μm by a Teflon tape gasket. The reactant gas mixture consisting of 80% O_2 and 20% argon flowed through the reactor with a rate of ~0.5 mL/min (corresponding to a space velocity of 1500 h^{-1}) via a single 10 μm outlet hole in the silicon plate. The reactor volume was approximately 20 mm^3 and was filled with catalyst powder. The UV source used was a 150 W Xe arc lamp focused on the reactor, with an intensity of 100 mW/cm^2. The exhaust gas was examined using mass spectrometry.

Results and Discussion

Preparation and Characterization of Mesoporous Titania. In this work the preparation of mesoporous titania with incorporated silver has been the focus. The preparation was carried out in two steps, the first being the synthesis of the mesoporous titania and the second the incorporation of silver into the mesostructure. It has been shown that the structure of the mesostructured material (cubic, hexagonal, or lamellar) is dictated by the relative volumes of the components in the synthesis solution, and that the binary water surfactant phase diagram can be used to predict the outcome of the synthesis.[41,46] More specifically, it is the relative volumetric fraction of the inorganic material, which in this case is the titania precursor together with the hydrochloric acid, and surfactant, in this case P123, that determines which structure is formed. The regimes where the mesostructures are present correspond closely to the ones observed in the binary P123−water system,[47] which can thus be used for predictive synthesis of a specific mesostructure. In this work focus has been on the cubic and hexagonal phases. The titania precursor used was an alkoxide. To be able to make ordered material of such a reactive species, it is necessary to control the condensation rate, which can be done by adjusting the pH.[48] Here we employed very low pH (pH < 0) to reduce the condensation rate. When making the mesoporous thin film, one starts by mixing the precursor with acid to initiate hydrolysis and hinder condensation; this prehydrolysate is then added to the structure-directing surfactant dissolved in ethanol. Since the concentration of the surfactant is far below the phase boundary for liquid crystalline phases, the viscosity of the mixture is relatively low, making it possible to form thin films. After dip coating, a range of processes take place. The solvent evaporates, resulting in higher surfactant concentration that eventually leads to formation of a liquid crystal, the pH is increased due to evaporation of hydrochloric gas, and the titania precursor starts to condense and polymerize into a titania gel. This course of events is controlled by the speed of

(42) Huang, M. H.; Choudrey, A.; Yang, P. *Chem. Commun.* **2000**, 1063.
(43) Larson, A. C.; Dreele, R. B. V. *GSAS Reference Manual*; 1994.
(44) Howard, C. J.; Sabine, T. M.; Dickson, F. *Acta Crystallogr.* **1991**, *B47*, 462.
(45) Mills, A.; Elliott, N.; Parkin, I. P.; O'Neill, S. A.; Clark, R. J. *J. Photochem. Photobiol., A* **2002**, *151*, 171.
(46) Klotz, M.; Ayral, A.; Guizard, C.; Cot, L. *J. Mater. Chem.* **2000**, *10*, 663.
(47) Holmqvist, P.; Alexandridis, P.; Lindman, B. *J. Phys. Chem. B* **1998**, *102*, 1149.
(48) Livage, J.; Henry, M.; Sanchez, C. *Prog. Solid State Chem.* **1988**, *18*, 259.

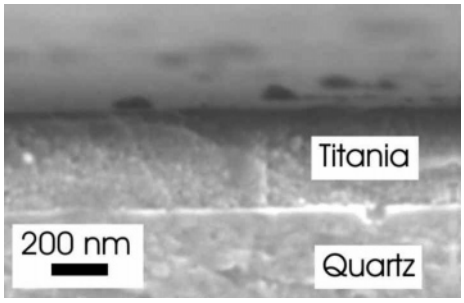

Figure 1. SEM micrograph showing mesoporous titania supported on a quartz slide. The shown film is on cubic titania extracted from the solution at a rate of 1 mm/s. The film is calcined at 400 °C, and its thickness is approximately 350 nm.

evaporation. Sanchez et al. have made several contributions to the understanding of this process and showed the great importance of the relative humidity in the synthesis of thin films.[49,50] In our case it was sufficient to work under ambient laboratory conditions during the dip coating. The thickness of the film is dependent on the slide pulling rate and the surfactant concentration. The film obtained in working with the cubic phase recipe and a pulling rate of 1 mm/s was approximately 350 nm after calcination at 400 °C as shown in Figure 1. The procedure for aging the film has been proven to influence the formed structure, but no detailed investigation of the aging time was performed in this study since it was found that 24 h of aging at ambient temperature was sufficient to get a highly ordered film. During the heat treatment, several mechanisms are active at the same time.[49,50] The titania cross-links and starts to crystallize, and at the same time the surfactant is calcined away, leaving a meso-ordered titania material. A critical step has been shown to be the calcination temperature and time.[49,50] Since anatase crystallites are formed in the titania walls of the mesostructure during heat treatment, they will destroy the meso-order if they grow too large. However, a crystalline material is desired for its material properties. Hence, there is a window during the heat treatment where the crystallites are formed, but where their size is small enough not to influence the ordered mesostructure. This window depends on which structure is targeted (e.g., cubic or hexagonal), making it difficult to make these mesostructures with the same amount of crystallinity. Alberius et al.[41] showed that the mesostructured order for the hexagonal structure could only be retained up to about 250 °C whereas the cubic phase could be maintained up to about 400 °C. As a consequence, the cubic phase contains more crystallites than the hexagonal phase. Since the desired form of titania for photocatalytic reactions is the crystalline form, the temperatures applied were as close as possible to the border of the material collapse.

The formed material was characterized by XRD at low diffraction angles, to study the long-range meso-order, as well as at higher angles, to characterize the crystallinity. The low-angle one-dimensional X-ray diffractogram shown in Figure 2 is in agreement with the distorted cubic phase.[41,49,50]

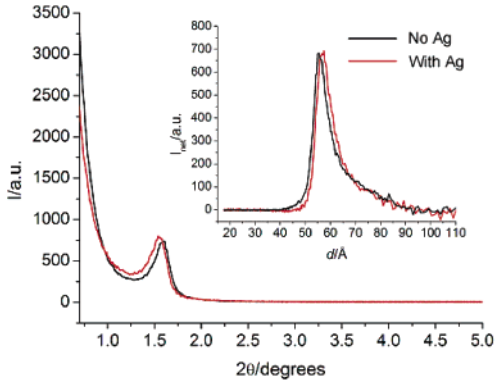

Figure 2. Low-angle X-ray diffractogram for a cubic mesoporous titania thin film after calcination at 400 °C for 4 h both without and with subsequent silver nanoparticle incorporation. The inset shows the background-corrected signals as a function of the *d* spacing.

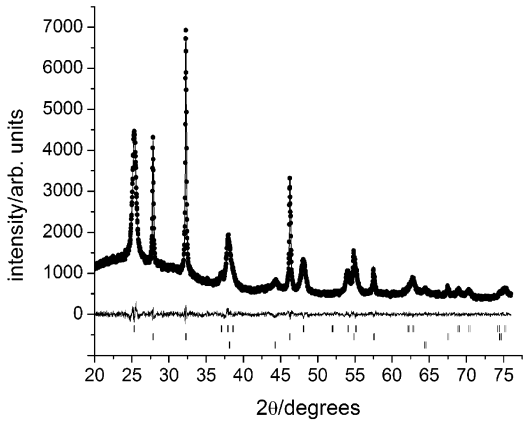

Figure 3. Wide-angle powder X-ray diffractogram for a cubic mesoporous titania film after calcination at 400 °C for 4 h and doped with silver. Circles represent the measured data, while the full line gives the Rietveld fit. The difference between the measurements and the model is given by the full line centered at zero intensity. The Bragg peaks are identified as anatase titania together with cubic silver and silver chloride. The peak positions are indicated by vertical bars in the order (from top to bottom) anatase, silver chloride, and cubic silver.

From the wide-angle powder X-ray diffractogram shown in Figure 3 the peaks for the titania can be identified as the anatase polymorph of titania. Silver and silver chloride are also present in the diffractogram as will be discussed further later in the paper. No rutile was found in the material. Further, the width of the peaks shows us that the titania particles are relatively small in size: from the Rietveld whole pattern refinement an apparent average particle size of about 15 nm was obtained. As stated earlier, both glass and quartz were used as film supports. During the low-angle X-ray characterization of materials made on the different supports, it appeared that the films made on quartz were more meso-ordered than the ones made on ordinary glass slides. This was observed as more intense peaks at low angles as well as the appearance of additional meso-order peaks at higher angles in the diffraction spectra of the films deposited on quartz. The origin of this difference is not yet understood, but we believe it to be due to the more well-defined surface of the quartz, which may play a role during film formation. Even if quartz was the preferred support, glass supports did give highly ordered material. The structure of the film material was studied more thoroughly using TEM, and typical micrographs of the mesoporous titania synthesized

(49) Crepaldi, E. L.; Soler-Illia, G. J. d. A.; Grosso, D.; Cagnol, F.; Ribot, F.; Sanchez, C. *J. Am. Chem. Soc.* **2003**, *125*, 9770.
(50) Grosso, D.; Solar-Illia, G. J. d. A.; Crepaldi, E. L.; Cagnol, F.; Sinturel, C.; Bourgeois, A.; Brunet-Bruneau, A.; Amenitsch, H.; Albouy, P. A.; Sanchez, C. *Chem. Mater.* **2003**, *15*, 4562.

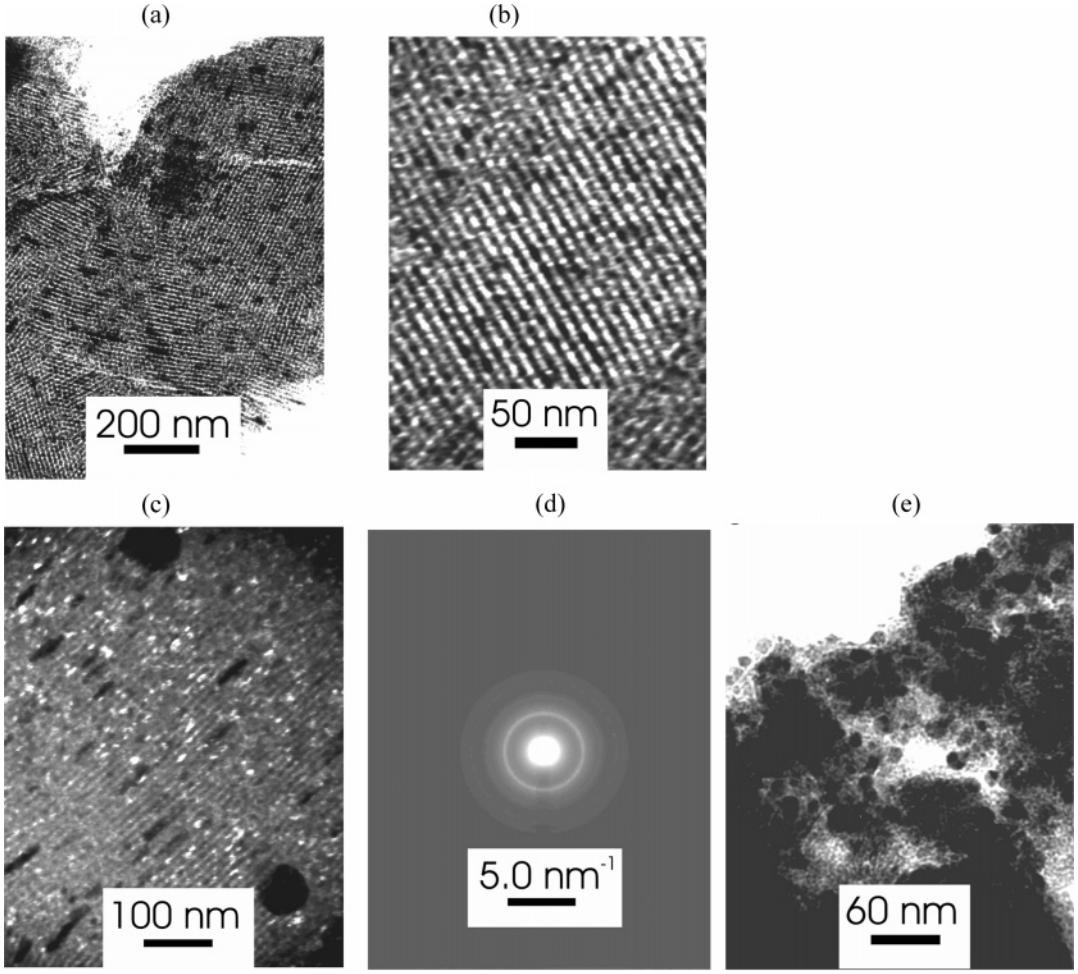

Figure 4. TEM micrographs of mesoporous titania with incorporated silver. (a) and (b) show the highly ordered mesoporous cubic structure of titania at different magnifications. The dark spots are silver particles situated within the titania. (c) shows a dark field micrograph taken on mesoporous cubic titania. Here the bright spots are titania crystallites and the very dark spots are silver nanoparticles. The crystalline structure of the titania is anatase as indicated by the electron diffraction pattern in (d). (e) shows a micrograph taken on a hexagonal film with no long-range order present and with the silver particles being larger in size than those in the cubic structure.

on quartz are shown in Figure 4. As seen from these images (Figure 4a,b), the cubic material is highly ordered (silver is also present in the micrographs as will be discussed later in the paper). It has previously been shown that dark field TEM can be used to highlight titania crystallites in an amorphous matrix.[51] A dark field micrograph based on the anatase (101) reflection (Figure 4d) is shown in Figure 4c. Since a single reflection is used in dark field imaging, only those particles with the corresponding Bragg angle toward the electron beam are highlighted; consequently, a precise measure of the particle size cannot be obtained by this method. This also affects the apparent crystallite concentration of the sample. For the hexagonal mesostructure one could see that the structure was ordered after the heat treatment (250 °C, 4 h) according to low-angle X-ray diffraction (not shown), but the presence of anatase crystallites could not be observed by electron diffraction in TEM. Heat treatment at 400 °C did give anatase but also resulted in disappearance of the meso-order of the hexagonal sample.

Incorporation of Silver. The combination of titania and silver has proven to be a good candidate material for photocatalytic reactions. Titania in a mesoporous structure is interesting in the sense that it generally has a high surface area in a continuous structure rather than in discrete particles. This continuity can be expected to make the electron transfer within the material easier, resulting in higher activity. It has been shown that if the silver is in the form of nanoparticles, which results in a large specific surface area as well as unique optical and electronic properties, it can enhance photocatalytic activity in a most effective way.[15] In the present work, silver ions were adsorbed on the titania surface and later reduced under controlled conditions to yield a silver/titania catalyst. A mixture of $AgNO_3$, ethanol, and water, which has been used for making silver nanowires within mesoporous silica,[42] was applied because of its penetrating capabilities. During impregnation, which was done for 24 h at room temperature, a difference between the hexagonal and cubic mesoporous titania was observed. The hexagonal sample turned (more or less) black during the impregnation, while the cubic sample turned pale gray, indicating that the silver ions were reduced in the hexagonal case but negligibly so

(51) Yang, P.; Zhao, D.; Margolese, D. I.; Chmelka, B. F.; Stucky, G. D. *Nature* **1998**, *396*, 152.

in the cubic system. We believe that this difference is due to the lower calcination temperature of the hexagonal phase, which, at least in the 4 h calcination period at 250 °C, is not sufficient to burn away all the structure-directing surfactant. The surfactant is known to reduce silver ions,[52,53] and we suggest that the remaining surfactant contributed to reducing the silver ions. This reduction of the silver in the hexagonal sample caused by the surfactant led not only to the formation of silver but also to loss of the long-range order of the titania. Figure 4e shows a typical TEM micrograph for the hexagonal titania after the incorporation of silver. As can be seen there is no long-range order and silver is present as particles of approximately 20 nm diameter. The cubic structure was made at 400 °C, which led to a more complete removal of the surfactant, and an extra step had to be carried out for the reduction of the silver ions. TEM micrographs of the cubic mesoporous titania with silver incorporated are shown in Figure 4a,b. Here it is seen that the silver particles are situated within the titania framework and that they are smaller in size (~8 nm) than the silver particles in the hexagonal sample. The particle size obtained by XRD, 12.6(4) nm, is in fair agreement herewith. The incorporation of silver does not disrupt the meso-order as seen from the small-angle X-ray diffraction data in Figure 2. The observed shift in *d* spacing upon introduction of silver, from 5.66 to 5.56 nm, is insignificant when the difference in sample absorption is taken into account. The silver formation in the cubic structure is believed to by hindered by the titania framework, and thereby structure directed, to form nanoparticles of roughly the same size as the pores. The loading of the titania is estimated to be roughly 6% by PXRD. To study the existence of both silver and titania on the surface, XPS was performed on a cubic, a hexagonal, and a silver-loaded hexagonal film. Figure 5 shows both the survey (a) and the high-resolution (b, c) spectra. They are consistent with a single oxidation state of Ti, the chemical shift and line width being the same for the three investigated films. Hence, both silver and titania are present on the surface and are available for the photocatalytic reaction.

Photocatalytic Activity. The photocatalytic activity of three anatase samples was investigated. Two cubic meso-ordered titania materials, both calcined at 400 °C, one containing silver, were compared to a reference sample without meso-order or silver. The reference was prepared by calcination of the ordered titania at 600 °C instead of 400 °C, leading to larger anatase crystallites and loss of long-range order. Figure 6 shows the produced CO_2 as a function of UV illumination time for the three samples. All three samples showed photocatalytic activity for oxidation of stearic acid. As anticipated, the highly ordered cubic mesoporous titania was crystalline enough to be photoactive. From Figure 6 it can be seen that the shape of the curves for the cubic meso-ordered non-silver-containing sample and the reference sample resemble each other to a high extent, indicating that the same reaction mechanism occurs with these two samples. The differences in the produced amount

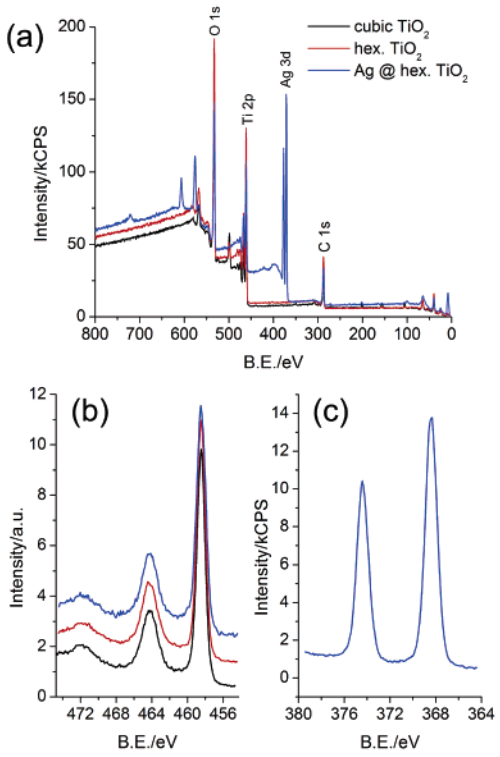

Figure 5. XPS analysis of as-prepared mesoporous titania samples with and without silver incorporated showing the (a) survey spectra, (b) high-resolution spectra for Ti, and (c) high-resolution spectra for Ag.

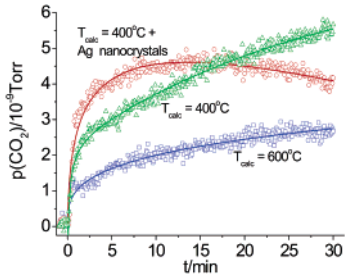

Figure 6. Results from the photocatalytic experiments showing the generation of CO_2 as a function of time upon UV illumination of mesoporous titania with stearic acid. Lines are guides to the eye. Key: red circles, silver-containing cubic mesoporous sample calcined at 400 °C; green triangles, cubic mesoporous sample calcined at 400 °C; blue squares, cubic mesoporous sample calcined at 600 °C (no longer ordered mesoporous).

of CO_2 for these two cases could be due to several factors, such as differences in stearic acid loadings, catalyst specific surface areas, irradiated sample volumes, or photocatalytic activity. In comparing the silver-containing sample with the non-silver-containing ones, a difference in the shape of the curves is seen. The most likely explanation for the observed difference is that the presence of silver facilitates decompositions via a different reaction path. Furthermore, the silver-containing titania has an apparent higher initial activity (higher initial slope of the curve). The drop in CO_2 formation for the silver-loaded sample after 17 min was not observed for the samples without silver. This difference can be due to (i) differences in stearic acid loadings or (ii) poisoning or more rapid deactivation of the silver-containing sample. The effect of silver addition is believed to cause an electron transfer between the titania and silver, whereby the photo-induced electron−hole pair of the titania is stabilized. It should also be noted that AgCl has been proven to be

(52) Andersson, M.; Alfredsson, V.; Kjellin, P.; Palmqvist, A. E. C. *Nano Lett.* **2002**, *2*, 1403.
(53) Liz-Marzán, L. M.; Lado-Touriño, I. *Langmuir* **1996**, *12*, 3585.

photocatalytically active due to the fact that silver clusters can be formed upon irradiation with UV light.[54] This should be taken into account since the silver-containing sample contains a relatively high amount of AgCl.

Conclusion

In this paper we report the synthesis of highly ordered mesoporous titania as a thin film with incorporated silver nanoparticles and its photocatalytic activity. The cubic structured mesoporous titania could be formed with a high content of nanocrystalline anatase with conservation of meso-order. Silver was incorporated by in situ heat induced reduction, and nanoparticles were formed within the meso-structure acting as a template. The formed material's photocatalytic activity was examined using degradation of stearic acid as a model reaction. It was shown that meso-ordered titania was photocatalytically active and that the activity was influenced by the presence of silver nanoparticles.

Acknowledgment. This work was financially supported by the Swedish Foundation for Strategic Research (SSF) through its Colloid and Interface Technology program together with a grant from the Bengt Lundqvist Foundation. A.E.C.P. acknowledges support from the Competence Centre for Catalysis, which is financially supported by the Swedish National Energy Administration and the member companies: AB Volvo, Johnson Matthey CSD, Saab Automobile AB, Perstorp AB, Albemarle Catalysts, MTC AB, and Swedish Space Corp.

CM0485761

(54) Currao, A.; Reddy, V. R.; Calzaferri, G. *ChemPhysChem* **2004**, *5*, 720.